Hyperactivation of the Insulin-like Growth Factor Receptor I Signaling Pathway Is an Essential Event for Cisplatin Resistance of Ovarian Cancer Cells

Niels Eckstein,[1] Kati Servan,[1] Barbara Hildebrandt,[2] Anne Pölitz,[2] Georg von Jonquières,[1] Sybille Wolf-Kümmeth,[1] Inge Napierski,[1] Alexandra Hamacher,[1,3] Matthias U. Kassack,[3] Jan Budczies,[4] Manfred Beier,[2] Manfred Dietel,[4] Brigitte Royer-Pokora,[2] Carsten Denkert,[4] and Hans-Dieter Royer[1]

[1]Center of Advanced European Studies and Research (caesar), Bonn, Germany; [2]Institute of Human Genetics and Anthropology and [3]Pharmaceutical Biochemistry, Institute of Pharmaceutical and Medicinal Chemistry, Heinrich-Heine University of Düsseldorf, Düsseldorf, Germany; and [4]Institute of Pathology, Charité University Hospital, Berlin, Germany

Abstract

Platinum plays a central role in the therapy of ovarian cancer, and the emergence of platinum resistance is a major obstacle for clinical management of the disease. We treated A2780 ovarian cancer cells by weekly cycles of cisplatin over a period of 6 months and unveiled that enhanced insulin-like growth factor I receptor (IGF-IR) expression and autocrine IGF-I are associated with hyperactivation of the IGF-IR and phosphatidylinositol-3-OH kinase (PI3K) pathways in cisplatin-resistant cells. *IGF-IR* expression levels increased during treatment cycles and correlated with cisplatin resistance. Purified IGF-I induced cisplatin resistance in diverse ovarian cancer cell lines, and small molecule inhibitors proved that IGF-IR and PI3K are essential for cisplatin resistance. Similar results were obtained with BG-1 ovarian cancer cells. Cytogenetic and array comparative genomic hybridization analyses revealed selection and *de novo* formation of chromosomal alterations during resistance development. An analysis of gene expression profiles of primary ovarian carcinomas identified the regulatory subunit *PIK3R2* of PI3-kinase as a significant negative prognosis factor for ovarian cancer. We conclude that targeting the IGF-IR and the PI3K pathways is a promising new strategy to treat cisplatin-resistant ovarian carcinomas. [Cancer Res 2009;69(7):2996–3003]

Introduction

In the Western world, epithelial ovarian cancer is the most lethal gynecologic cancer (1). Epithelial ovarian cancer is a chemosensitive neoplasm, with initial overall response rates to systemic therapy exceeding 80% when integrated with cytoreductive surgery (1). Platinum-based chemotherapy has improved outcomes in women with ovarian cancer in the last 25 years (2). Primary postoperative chemotherapy has evolved from single alkylating agents to cisplatin and cisplatin-based combinations, followed by incorporation of paclitaxel and substitution of carboplatin for cisplatin (1). Thus, platinum plays a central role in the therapy of ovarian cancer, and the emergence of platinum resistance is a major obstacle for clinical management of the disease (3). It is evident from the literature that cellular resistance to cisplatin is incompletely understood and the current state of the art is insufficient for translation into clinical applications (4–6). Ovarian cancer patients are treated by multiple cycles of postoperative chemotherapy (3), and the emergence of resistance to chemotherapy is a process that ranges from months to years (1, 3).

To mimic this process in tissue culture, we developed a novel strategy and investigated the development of cisplatin resistance in human breast cancer cells (7). It was the aim of this work to use this strategy to study cisplatin resistance in A2780 ovarian cancer cells that are sensitive for chemotherapeutic agents (8, 9). They are wild-type with respect to p53 and *RAS* (10, 11). Previously, cisplatin-resistant A2780 cells ($A2780^{CP}$) were generated by exposure to increasing concentrations of cisplatin (9). Here, we used weekly cycles of an IC_{50} dose of cisplatin and monitored the dynamics of resistance development over a period of 24 weeks. We report that hyperactivation of the insulin-like growth factor I (IGF-I) receptor pathway is a crucial step for the development of cisplatin resistance in A2780 ovarian cancer cells. We have thus identified a mechanism for cisplatin resistance in ovarian cancer, which is distinct from the one in breast cancer where amphiregulin-dependent activation of the epidermal growth factor receptor signaling pathway provoked resistance (7). Hence, cell type and tumor type–specific mechanisms of chemotherapy resistance have to be taken into account for the development of effective therapies.

Materials and Methods

Cell culture and preparation of cell lysates. HEY, OVCAR-8, SKOV-3, BG-1, and A2780 ovarian cancer cells were obtained from a cell line repository (JJ Hernando, Womans Hospital, University of Bonn, Germany). $A2780^{CP}$ cells were from the European Collection of Cell Culture. Cells were cultivated in RPMI 1640 (Biochrom) containing 10% FCS, 100 IU/mL penicillin, and 100 μg/mL streptomycin. The preparation of whole cell lysates has been described (7).

Signaling pathway analysis. The functional status of signaling pathways was measured by Proteome Profiler human phospho–receptor tyrosine kinase (RTK) and human phospho–mitogen-activated protein kinase (MAPK) antibody arrays (R&D Systems) as reported (7). The IGF-I ELISA procedure followed a protocol from the producer (R&D Systems).

Analysis of IGF-I receptor expression. For immunoblotting, standard procedures were used. To detect the IGF-I receptor (IGFI-R), the affinity-purified AF-305-NA antibody and the HAF 109 donkey anti-goat IgG–horseradish peroxidase antibody (R&D systems) were used. Immunoblots

Note: Supplementary data for this article are available at Cancer Research Online (http://cancerres.aacrjournals.org/).

Requests for reprints: Hans-Dieter Royer, Center of Advanced European Studies and Research, Ludwig-Erhard-Allee 2, 53175 Bonn, Germany. Phone: 49-228-9656-168; Fax: 49-228-965-6201; E-mail: royer@caesar.de.

doi:10.1158/0008-5472.CAN-08-3153

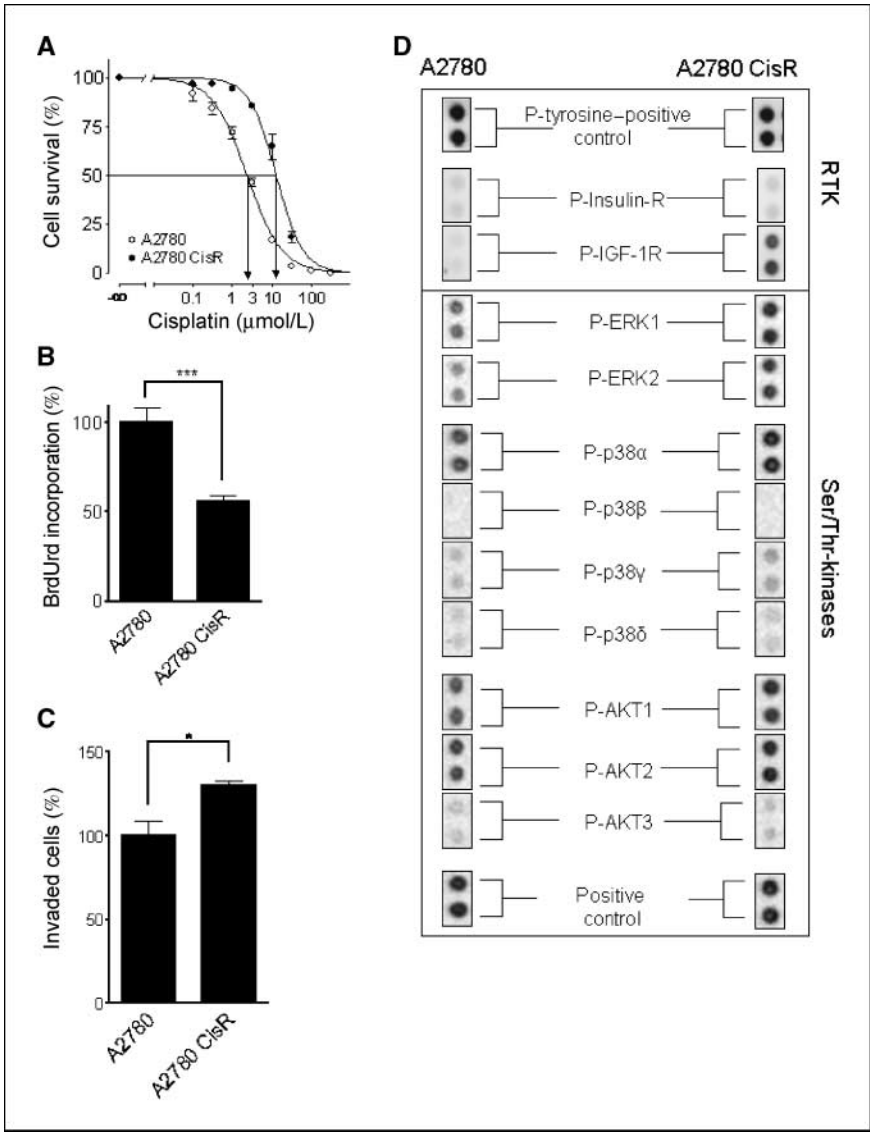

Figure 1. Generation and characterization of cisplatin-resistant A2780 cells. *A,* cisplatin resistance was measured by MTT assays (7). A2780 cells (*open circles*) and A2780 CisR cells (*filled circles*). The factor of resistance was calculated by dividing the IC_{50} concentrations from resistant cells by IC_{50} concentrations from nonresistant cells. *Arrows,* IC_{50} concentrations of cisplatin. *B,* decreased proliferation of cisplatin-resistant A2780 CisR cells. The proliferation rates were determined by a BrdUrd incorporation assay. A2780 cells (*left bar*) and A2780 CisR cells (*right bar*). Significant differences are indicated by asterisks ($n = 4$, Student's t test; ***, $P < 0.001$). *C,* invasive ability of A2780 CisR cells. To determine invasion abilities, we used a Matrigel invasion assay. Significant differences are indicated by asterisks ($n = 4$, Students t test; *, $P < 0.05$). *D,* hyperactivation of the IGF-IR and PI3K pathways in A2780 CisR cells. Human phospho-RTK antibody arrays were used to measure RTK phosphorylation, and human phospho-MAPK antibody arrays were used to measure phosphorylation of MAP- and AKT-kinases. Phosphorylation sites detected by this assay are listed (Supplementary Table S1).

were developed with the enhanced chemoluminescence system (Amersham Biosciences).

Matrigel invasion and BrdUrd proliferation assay, 3-(4,5-dimethylthiazol-2-yl)-2,5-diphenyltetrazolium bromide cell growth assay, and signaling inhibitors. To determine invasive potential of A2780 CisR cells, the CytoSelect assay (Cell Biolabs Inc.) was used (7). The BrdUrd proliferation assay (Roche Applied Science) was done as described (7). For 3-(4,5-dimethylthiazol-2-yl)-2,5-diphenyltetrazolium bromide (MTT) assays, we followed our published protocol (7). Signaling inhibitors LY294002 (5 μmol/L), U0126 (2.5 μmol/L), Wortmannin (30 nmol/L), AG 1024 (1 μmol/L; Sigma-Aldrich), or IGFBP 4 (0.1 μmol/L; R&D Systems) were added to the tissue culture medium 1 h before the addition of cisplatin.

Cytogenetic and fluorescence *in situ* hybridization analyses. Metaphase chromosomes were prepared following standard procedures. Giemsa karyotypes were generated according to International System for Human Cytogenic Nomenclature (12), and fluorescence *in situ* hybridizations (FISH) were performed as described (13). PAC/BAC probes were from (Genome Systems; imaGenes). GS-1186-B18 (3p, PAC), GS-1061-L1 (20p, PAC), RP11-1129-O4 (1p, BAC), and GS-580-L5 (8p, PAC; ref. 14) were labeled with cyanine 3-dUTP (Cy3) or cyanine 5-dUTP (Cy5) so that two probes could be visualized in one combined hybridization.

Array comparative genomic hybridization and data analysis. DNA was isolated with the Qiagen Mini kit (tissue protocol) and digested with *Alu*I and *Rsa*I (Promega). Purified DNA (1.5 μg of each) was labeled with Cy5 (A2780 cells) or Cy3 (A2780 CisR cells) using the Genomic DNA labeling kit Plus (Agilent). Cy5- and Cy3-labeled samples were combined and hybridized for 40 h at 65°C with the Human Genome Comparative Genomic Hybridization (CGH) Microarray 244A (Agilent). Data analysis was described previously (15). For better interpretability, the resulting data set was transformed from the original base 10 to base 2 log-ratios. CGH-plots were created for visual inspection using two software packages based on R: Bioconductor's array comparative genomic hybridization (aCGH) package[5] for genome wide plots, and the GLAD package for chromosome specific plots with automatic break point detection (16).

Quantification of *IGF-IR* mRNA by real-time reverse transcription-PCR. Our reverse transcription-PCR (RT-PCR) protocol has been published (7). The primers used were *IGF-IR* forward (5′-GAAGTGGAACCCTCCCTCTC-3′) and *IGF-IR* reverse (5′-CTTCTCGGCTTCAGTTTTGG-3′); *β-actin* forward (5′-AGAAAATCTGGCACCACACC-3′) and *β-actin* reverse (5′-CAGAGGCGTACAGGGATAGC-3′). The *IGF-IR* mRNA concentration was normalized to *β-actin* mRNA.

[5] http://www.bioconductor.org

Data analysis. Indicated are the mean values ± SE. Concentration effect curves were fitted to the data points by nonlinear regression analysis using the four-parameter logistic equation (GraphPad Prism).

Statistical methods. Assays were performed at least in triplicate. Statistical significance was assessed by two-tailed Student's *t* test for single comparison and ANOVA for multiple comparisons, respectively.

Results

Generation and characterization of cisplatin-resistant A2780 ovarian cancer cells. A2780 cells were exposed to weekly cycles (4 hours) of 2 μmol/L cisplatin over a period of 24 weeks. The resistance factor after 24 treatment cycles was calculated as 5.8 (**, $P < 0.01$; Fig. 1*A*). Cisplatin-resistant cells were denoted A2780 CisR and they remained resistant after cultivation in drug-free media for at least 4 months (Supplementary Fig. S1). A2780 CisR cells are characterized by reduced proliferation rates (Fig. 1*B*) and an increased ability to degrade and, thus, invade the matrix of a reconstituted basement membrane (Fig. 1*C*). Hence, cisplatin resistance and tumor cell aggressiveness are linked to each other. To investigate whether A2780 CisR cells developed cross-resistance, we analyzed the anthracycline doxorubicin (Supplementary Fig. S2) and measured a resistance factor of 4.2.

Hyperactivation of the IGF-IR pathway in A2780 CisR ovarian cancer cells. Next, we analyzed the functional status of RTKs and downstream signaling pathways in A2780 CisR cells using antibody arrays. We find a selective phosphorylation of the IGF-IR (Fig. 1*D*). The IGF-IR signaling pathway is connected to three major MAPK pathways (reviewed in ref. 17). We used a human phospho-MAPK antibody array (7; Supplementary Table S1) and detected moderate extracellular signal-regulated kinase (ERK)1 and ERK2 phosphorylation in A2780 cells, which is markedly increased in A2780 CisR cells (Fig. 1*D*). In contrast, the phosphorylation of c-Jun NH_2-terminal kinases (18) did not change (data not shown). The p38 MAPK module consists of four isoforms and we detected p38 α phosphorylation in A2780 cells, which is increased in A2780 CisR cells (Fig. 1*D*). The IGF-IR pathway is also linked to the phosphatidylinositol-3-OH kinase (PI3K)/AKT pathway by insulin receptor substrate 1 (reviewed in ref. 17). PI3K regulates the translocation of AKT-kinase to the cell membrane where it becomes phosphorylated at S473 by phosphoinositide-dependent kinase 1 and the rictor–mammalian target of rapamycin complex (19). AKT1 and AKT2 are moderately phosphorylated in A2780 cells and phosphorylation is strongly increased in A2780 CisR cells. These data show that hyperactivation of the IGF-IR and PI3K signaling pathways is associated with cisplatin resistance.

Temporal dynamics of *IGF-IR* gene expression correlate with cisplatin resistance in A2780 ovarian cancer cells. Cisplatin resistance development was monitored by MTT assays (Fig. 2*A*). The cells developed cisplatin resistance after 6 treatment cycles, which steadily increased up to treatment cycle 12. We also measured the levels of *IGF-IR* mRNA (Fig. 2*B*). A comparison of the dynamics of cisplatin resistance development (Fig. 2*A*) and the dynamics of *IGF-IR* gene expression (Fig. 2*B*) reveals an almost identical curve progression. This result shows that *IGF-IR* expression levels correlate with the extent of cisplatin resistance of A2780 ovarian cancer cells.

Hyperactivation of the IGF-IR pathway is associated with enhanced IGF-IR expression and constitutive IGF-I secretion. We determined IGF-IR expression by immunoblotting using an antibody specific for the extracellular domain of the IGF-IR

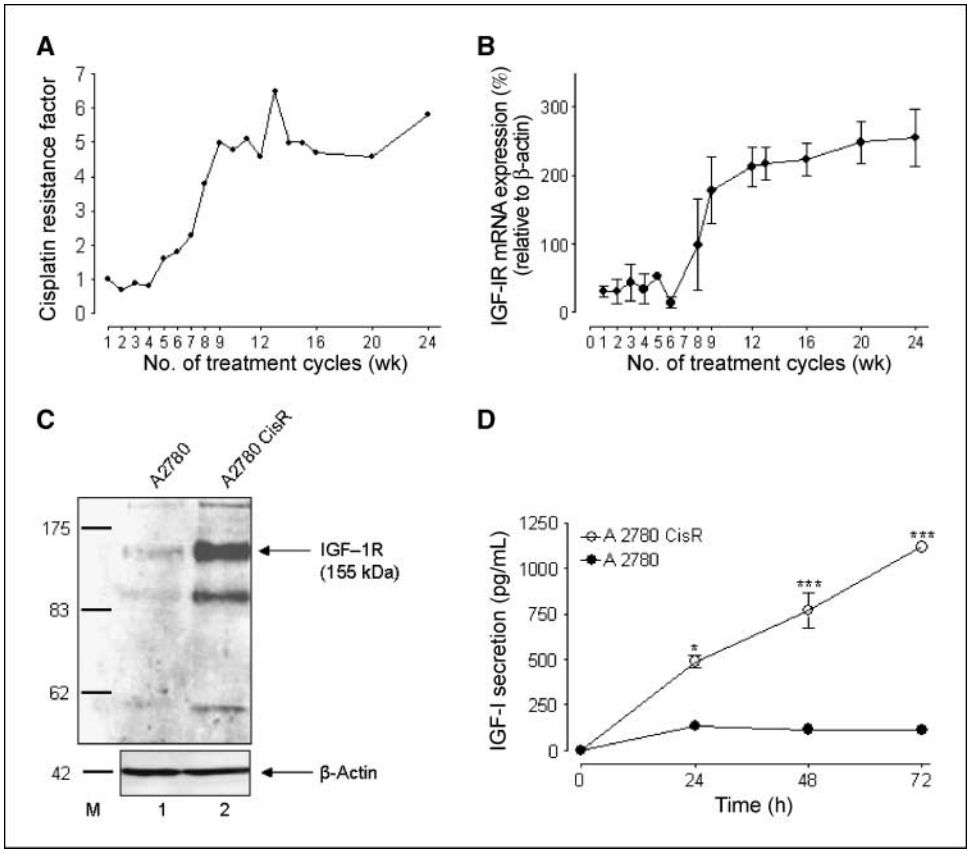

Figure 2. Development of an autocrine IGF-I loop in cisplatin-resistant ovarian cancer cells. *A,* dynamics of cisplatin resistance development. A2780 cells were treated by weekly cycles of cisplatin. The factor of resistance was calculated by dividing IC_{50} values at each time point with the IC_{50} value from control cells. *B, IGF-IR* mRNA expression in the course of cisplatin resistance development. *IGF-IR* mRNA levels were measured by real-time quantitative RT-PCR. *C,* enhanced expression of the IGF-IR in A2780 CisR cells. *Arrow,* the position of IGF-IR on the immunoblot. *M,* molecular weight marker. *D,* constitutive secretion of IGF-I from A2780 CisR cells. To quantify secreted IGF-I, cell culture supernatants from A2780 CisR and A2780 cells were analyzed by an IGF-I ELISA ($n = 3$; *, $P < 0.05$; ***, $P < 0.001$).

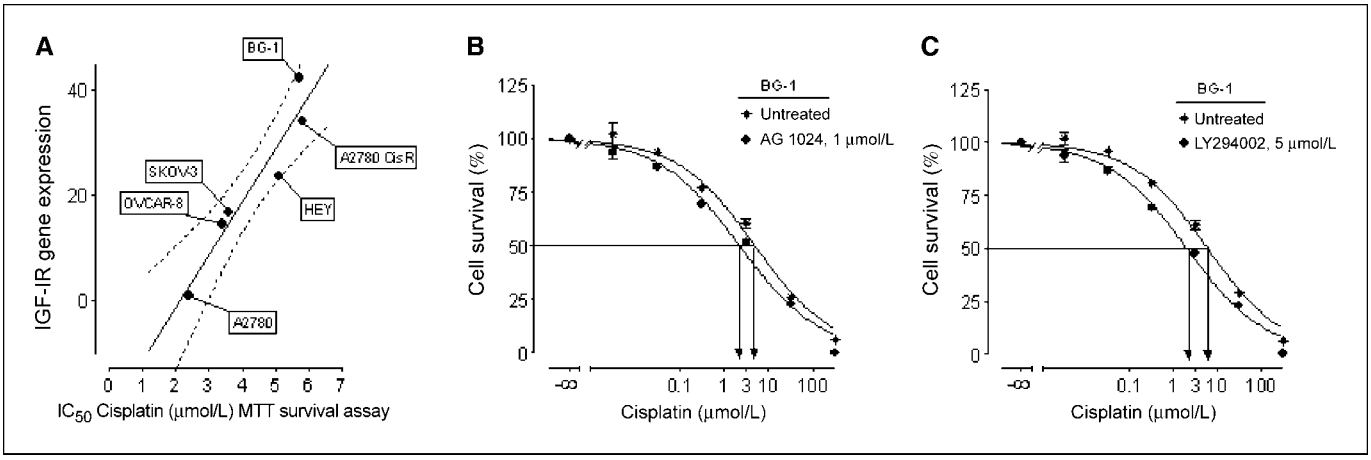

Figure 3. The IGF-IR signaling pathway determines cisplatin resistance in ovarian cancer cells. *A, IGF-IR* expression in diverse human ovarian cancer cells correlates significantly with cisplatin resistance. Cisplatin IC_{50} values from MTT assays were correlated with *IGF-IR* gene expression. The correlation coefficient was calculated 0.956 (*, $P = 0.0224$). *Dotted line,* 95% confidence interval. *B,* effect of the IGF-IR signaling pathway for the cisplatin-resistant phenotype of BG-1 ovarian cancer cells. BG-1 ovarian cancer cells were cultivated in the presence of AG 1024, which inhibits IGF-IR tyrosine kinase activity (*filled circles*), medium control (*). *Arrows,* IC_{50} concentrations of cisplatin for AG 1024 (*left arrow*) and medium control (*right arrow*). *C,* IGF-IR signaling through the PI3K pathway is essential for cisplatin resistance in BG-1 ovarian cancer cells. Cisplatin resistance of BG-1 cells after cultivation in the presence of LY294002, which inhibits PI3K activity. *Arrows,* IC_{50} concentrations of cisplatin for LY294002 and medium control.

(Fig. 2*C*). A2780 cells express very low levels of the IGF-IR, which are strongly enhanced in A2780 CisR cells. The same result was obtained by immunofluorescence analysis (Supplementary Fig. S3). Next, we investigated the status of IGF-I. To measure IGF-I in tissue culture supernatants, we used a sandwich ELISA (Fig. 2*D*) and detected constitutive IGF-I secretion from the resistant cells. Exposure of A2780 CisR cells to cisplatin or serum deprivation did not affect IGF-I secretion (data not shown). Thus, increased IGF-IR expression in combination with constitutive IGF-I secretion provides a mechanism for hyperactivation of the IGF-IR pathway in cisplatin-resistant ovarian cancer cells.

IGF-IR signaling through the PI3K pathway is crucial for cisplatin resistance. To determine the relevance of IGF-IR and PI3K signaling pathways for cisplatin resistance, we used specific inhibitors. We applied IGF binding protein-4 (IGFBP-4), which is a functional antagonist of IGF-I (reviewed in ref. 20), and determined IC_{50} values of cisplatin dose response curves. IGFBP-4 sensitized A2780 CisR cells significantly (Supplementary Table S2). Likewise, AG 1024, a tyrosine kinase inhibitor that selectively inhibits the IGF-IR sensitized the resistant cells significantly. Next, we used the PI3K inhibitors LY294002 and Wortmannin. These inhibitors efficiently sensitized A2780 CisR cells to cisplatin. As IGFBP-4, LY294002, and Wortmannin had almost identical effects, we conclude that IGF-IR–dependent signaling through the PI3K pathway is responsible for cisplatin resistance. In contrast, the ERK1/2 signaling pathway is not involved as inhibition of ERK1/2 signaling by the MAP/ERK kinase 1/2 inhibitors U0126 and PD98059 did not affect cisplatin resistance (Supplementary Table S2).

***IGF-IR* expression and cisplatin resistance in diverse human ovarian carcinoma cell lines.** Next, we measured *IGF-IR* mRNA expression levels and determined cisplatin resistance in a panel of ovarian cancer cell lines (Fig. 3*A*). SKOV-3 and OVCAR-8 are derived from metastatic tumors of patients previously treated with chemotherapy (21, 22). HEY was derived from a peritoneal deposit of a patient with a moderately differentiated papillary cystadenocarcinoma (23), and BG-1 was derived from the solid primary tumor tissue from an untreated patient with stage III, very poorly differentiated ovarian adenocarcinoma (24). We correlated *IGF-IR* expression levels with IC_{50} values from MTT assays and found a correlation coefficient of 0.9534, which is statistically highly significant (**, $P = 0.0032$). Thus, the level of *IGF-IR* mRNA predicts the extent of cisplatin resistance in ovarian cancer cells.

To check whether IGF-IR signaling through the PI3K pathway effects cisplatin resistance of other ovarian cancer cell lines, we selected BG-1 cells that are cisplatin resistant. They express high levels of *IGF-IR* mRNA (Fig. 3*A*) and very high levels of IGF-IR protein (25). The IGF-IR inhibitor AG 1024 and the PI3K inhibitor LY294002 significantly sensitized BG-1 cells to cisplatin (Fig. 3*B* and *C*). These data show that the IGF-IR and PI3K pathways also mediate cisplatin resistance in another ovarian cancer cell line and thus are of more general importance.

IGF-I mediates a bystander effect for cisplatin resistance in diverse ovarian cancer cells. Because most ovarian cancers express the IGF-IR, we hypothesized that IGF-I secreted from cisplatin-resistant cells might mediate a bystander effect in ovarian cancer patients. To test this hypothesis, we used A2780 cells as an *in vitro* model and cultivated the cells in conditioned medium from A2780 CisR cells. After 3 days, the level of sensitivity to cisplatin did not change. However, after 8 days, A2780 cells developed a cisplatin-resistant phenotype with a resistance factor of 3.04 (Fig. 4*A*), which was fully reversible after cultivation in normal medium (data not shown). This shows that factors present in the conditioned medium initiated a process leading to cisplatin resistance, which is dependent on the continuous presence of these factors. To investigate the effect IGF-I, we cultivated A2780 cells in conditioned medium for 8 days in the presence of IGFBP-4, which antagonizes IGF-I. Under these conditions, no resistance to cisplatin developed (Fig. 4*B*). Identical results were obtained, when the cells were cultivated in the presence of a neutralizing IGF-I–specific antibody (data not shown). Next, we cultivated A2780 cells for 8 days in the presence of 0.1 μmol/L IGF-I and MTT assays revealed an IC_{50} value for cisplatin, which is similar to the one

obtained by conditioned medium (Fig. 4*C*). We also cultivated Hey, OVCAR-8, SKOV-3, and BG-1 ovarian cancer cells in the presence of 0.1 μmol/L IGF-I for 8 days and determined the IC_{50} values for cisplatin (Supplementary Table S3). The data show that cisplatin resistance was significantly increased in all cell lines. Hence, IGF-I secretion from cisplatin-resistant ovarian cancer cells will most likely exert a bystander effect for cisplatin resistance in women with ovarian cancer.

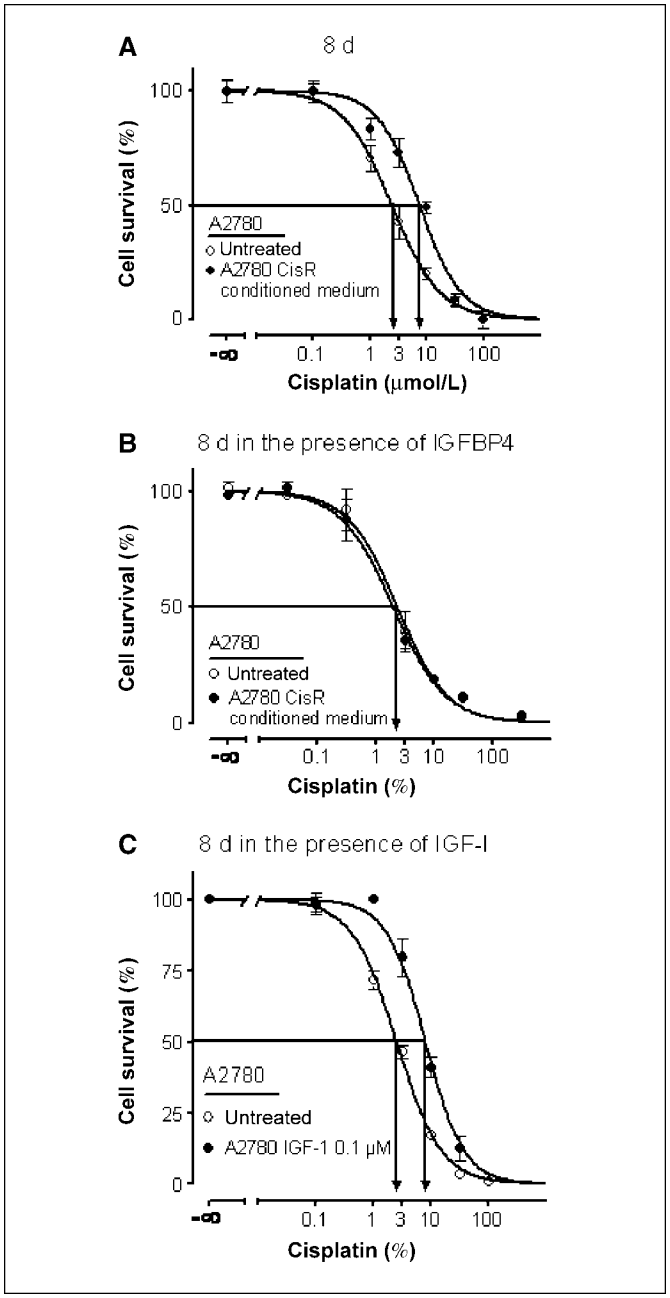

Figure 4. IGF-I mediates a bystander effect for cisplatin resistance in A2780 ovarian cancer cells. *A,* cisplatin resistance of A2780 cells after cultivation in A2780 CisR conditioned medium for 8 d. *Arrows,* IC_{50} concentrations of cisplatin for medium control and conditioned medium. *B,* IGFBP-4 revokes the bystander effect mediated by A2780 CisR–conditioned medium. Cisplatin resistance of A2780 cells after cultivation in conditioned medium for 8 d in the presence of IGFBP4. *Arrow,* IC_{50} concentration for cisplatin. *C,* emergence of cisplatin resistance in IGF-I treated A2780 ovarian cancer cells. Cisplatin resistance of A2780 cells after treatment with 0.1 μmol/L IGF-I. *Arrows,* IC_{50} concentrations of cisplatin.

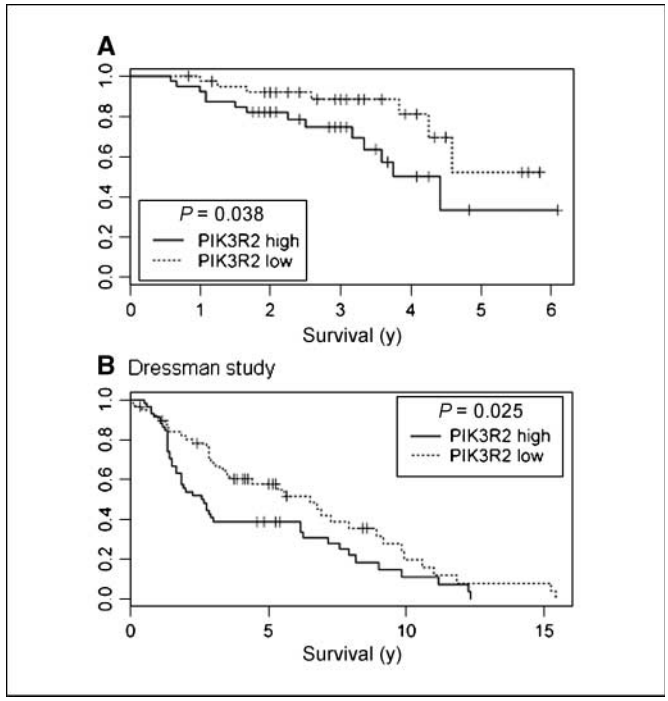

Figure 5. The regulatory subunit PIK3R2 of PI3K is a negative prognosis factor for ovarian cancer. The ovarian cancer cohort was divided into 40 tumors with high (*solid line*) and 40 tumors with low (*dotted line*) *PIK3R2* expression. *A,* Kaplan-Meier analysis shows a significant reduced overall survival for patients with high *PIK3R2* expression. *B,* validation of *PIK3R2* as negative prognosis factor in an independent study at another institution (Dressman study; ref. 28).

Identification of the regulatory subunit *PIK3R2* of PI3-kinase as prognostic biomarker for ovarian cancer. Next, we analyzed microarray data (Supplementary Materials and Methods) of a cohort of 80 ovarian cancer patients (Supplementary Table S4), whose clinical outcomes have been registered and asked whether the expression levels of genes from the IGF-IR and PI3K pathways would correlate with clinical outcome. We find that *PIK3R2* expression had a significant negative correlation ($P = 0.037$; Fig. 5*A*) and *AKT2* expression a borderline significant negative correlation ($P = 0.070$) with overall survival (data not shown). PIK3R2 is a regulatory subunit of PI3-kinase. It is interesting to note (Fig. 5*B*) that *PIK3R2* expression negatively correlated with clinical outcome ($P = 0.026$) in an independent study of 83 advanced-stage serous ovarian cancers (26).[6] As the above microarray data were from untreated tumors, additional studies with microarray data from ovarian cancer tissue after cisplatin treatment are necessary. However, patients with advanced disease do not routinely undergo surgery for additional tissue samples to be collected (27).

Selection and acquisition of structural genomic alterations in cisplatin-resistant ovarian cancer cells. It is unresolved whether selective or adaptive mechanisms contribute to cisplatin resistance. To address this issue, we applied cytogenetics, FISH, and aCGH. A2780 CisR cells had several chromosomal abnormalities in common with $A2780^{CP}$ cells (28) that were generated by increasing cisplatin concentrations (9) including monosomy of chromosome

[6] http://data.cgt.duke.edu/platinum.php

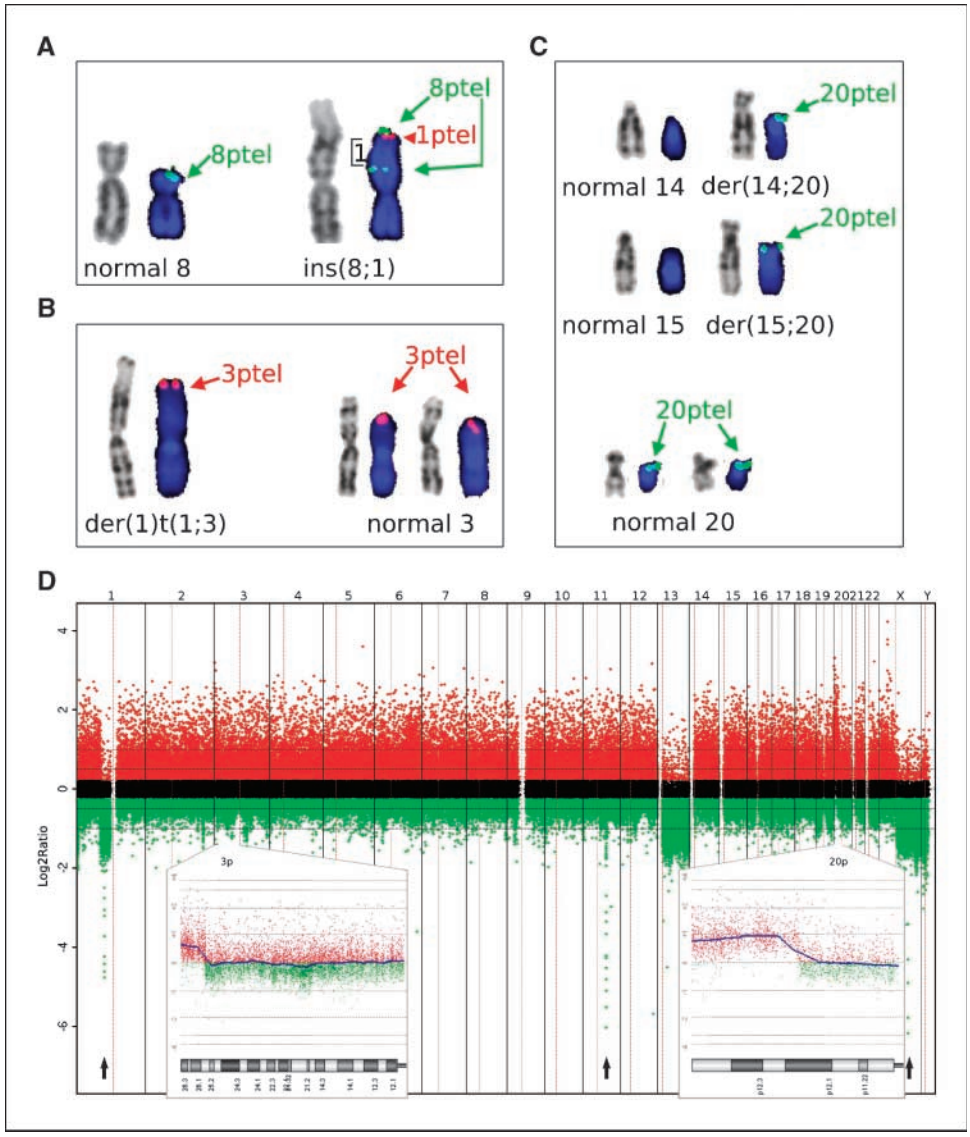

Figure 6. Selection and *de novo* acquisition of genomic alterations during cisplatin resistance development. *A,* description of the ins(8;1)(p22;p22p36). *Left,* the normal banding pattern of the ins(8;1) chromosome is shown and the FISH hybridization with a 8p (*green*) and a 1p (*red*) telomere probe. *B,* location of the three copies of chromosome 3p. The normal banding pattern is shown on the left for the der(1)t(1;3)(p36;p26), with the 3p telomere probe (red) at the tip of the chromosome. *C,* location of the four copies of chromosome 20. *Left,* the normal chromosomes 14 and 15 do not show a hybridization signal with the 20p telomere probe (*green*), whereas both derivative chromosomes 14 and 15 contain a 20p telomere signal on the p arm. *D,* whole genome profile of cisplatin-resistant A2780 CisR cells. Probes with $\log_2$-ratio >0.2 (gain; *red*), <−0.2 (loss; *green*), and between −0.2 and 0.2 (no change; *black*) are shown. *Insets,* a more detailed view of the gains on chromosomes 3p (*left*) and 20 p (*right*). The three arrows at the bottom of the figure mark the homozygous deletions on chromosome 1 (*left arrow*), 11 (*middle arrow*), and X (*right arrow*) with log ratios between −5, −6, and −7, respectively.

13. These are highlighted by boldface type in the karyotype formula. A2780 CisR cells exhibit additional chromosomal alterations (Fig. 6*A*–*C*). aCGH unveiled two larger gains of chromosome 3p (3p26) and 20p (20p12), which are shown as insets on the left (3p) and on the right (20p) in Fig. 6*D*. Several aberrations were verified by FISH and the final karyotype of A2780 CisR cells was compiled from aCGH, FISH, and conventional karyotype analysis:

44X,**der (X)t(X;1)(q12;q11)**, -1,der (1)t(1;3)(p36;p26),**der(6)t(1;6)(q21;q22)**, ins(8;1)(p22;p22p36),**-13**, der (14)t(14;20)(p12;p112.2), der(15)t(15;20)(p12;p12.2),add (22)(p11) [22].

Telomere probes from chromosome 8p (*green*) and 1p (*red*) showed that the der8 (28) contains a subtelomeric insertion of 1p22p36 splitting the telomere 8p (*green arrows*) and retaining the telomere 1p (*red arrow*; Fig. 6*A*). The copy number gain of 3p26 detected by aCGH showed a fold change of 1.5, which is explained by the fact that 3 copies were observed in FISH with a 3p telomere probe, 2 on the normal chromosome 3, and 1 on the der(1)t(1;3; Fig. 6*B, red arrows*). For the copy number gain of 20p12, a fold change of 1.99 was seen, which is explained by the fact that four copies were observed in FISH with a 20p telomere probe (Fig. 6*C*), 2 on the normal chromosome 20 (*bottom*), 1 on the der(14; top panel), and 1 on the der(15) middle (Fig. 6*C, green arrows*). Smaller aberrations identified by aCGH were three homozygous deletions (Fig. 6*D, arrows*), and several copy number gains and losses (Supplementary Table S5). Next, we investigated whether monosomy 13 was already present in nonresistant A2780 cells using FISH with two different probes from chromosome 13. Monosomy 13 was found in 2.1% of A2780 and 100% of A2780 CisR cells, demonstrating selection of this chromosomal alteration. In addition, 3 copies of 20p12 (Fig. 6*C*) were already present in 3.9% of A2780 cells and 1.5% had four copies. In contrast, the copy number gain of 3p26 in cisplatin-resistant cells (Fig. 6*B*) was undetectable in A2780 cells. Thus, A2780 cells with copy number gains of 20p12 were selected during cisplatin resistance development and the copy number gain of 3p26 is a *de novo* event.

Discussion

We used A2780 epithelial ovarian cancer cells as an *in vitro* model to investigate the dynamics of cisplatin resistance

development. We analyzed structural genomic alterations, gene expression, and the activities of selected signal transduction pathways. We clarified that the development of cisplatin resistance is associated with the selection of preexisting genomic alterations and the acquisition of *de novo* changes demonstrating that both selective and adaptive processes are linked to the development of cisplatin resistance.

We show here that hyperactivation of the IGF-IR signaling pathway is a crucial step for the development of cisplatin resistance of A2780 ovarian cancer cells. The IGF-IR is physiologically expressed in the ovary and the IGF-IR pathway is functional in human ovarian surface epithelial cells, which are the origin of most epithelial ovarian carcinomas (29–31). This explains why most ovarian carcinomas and ovarian cancer cell lines express the IGF-IR (32).

We worked out that IGF-IR–dependent signaling through the PI3K pathway mediates cisplatin resistance in A2780 CisR and BG-1 ovarian cancer cells, which indicates a more general relevance of this result. In this context, it is important to note that CAOV-3 and OVCAR-3 ovarian cancer cells, which are also resistant to cisplatin (22, 33), express autocrine IGF-I (34). Likewise, cisplatin-resistant SKOV-3 (22) and OVCAR-4 (35) cells express both IGF-I and the IGF-IR (36, 37). Taken together, these results provide strong evidence for an essential role of the IGF-IR signaling pathway for cisplatin resistance in ovarian cancer.

A2780 cells have been used before to create a series of cisplatin-resistant cell lines that were selected by chronic exposure of increasing cisplatin concentrations (9). aCGH analysis revealed common genomic alterations in A2780 CisR and $A2780^{CP}$ cells (28), which are highlighted by boldface type in the karyotype formula. However, A2780 CisR cells also display unique genomic alterations. This shows that A2780 cells react differently to distinct cisplatin treatment regimens. This is corroborated by the finding that IGF-IR phosphorylation is not elevated in $A2780^{CP}$ cells (Supplementary Fig. S4). Even so, the PI3K pathway is essential for cisplatin resistance in these cells. We noted increased AKT1 and AKT2 phosphorylation (Supplementary Fig. S4), and the PI3K inhibitor LY294002 sensitized $A2780^{CP}$ cells significantly to cisplatin (Supplementary Fig. S5).

To show the effect of our findings for ovarian cancer patients, it is necessary to validate the results in a clinical situation. This could be achieved by investigating ovarian carcinomas with an early relapse after chemotherapy. However, patients with advanced disease do not routinely undergo surgery for additional tissue samples to be collected (27), and this explains why the necessary tumor specimens are difficult to obtain. However, an extensive survey of published data revealed convincing evidence for a role of IGF-IR and PI3K signaling pathways in ovarian cancer patients. Ovarian cancer tissue samples express increased amounts of IGF-IR compared with normal ovarian tissues (38). The levels of IGF-IR are significantly higher in the tumors of patients with recurrent or persistent disease after chemotherapy (39). Recurrent or persistent tumors of this study were collected at second-look or subsequent laparotomy (39). Moreover, IGF-I peptide is increased in cyst fluids of epithelial ovarian cancer (40), and in the ascites of ovarian cancer patients (41). A clinical study unveiled that IGF axis gene expression patterns are prognostic of survival in epithelial ovarian cancer (42). Yet another clinical study showed that a high level of free IGF-I peptide was independently associated with the progression of ovarian cancer (43).

We report that IGF-IR–dependent signaling through the PI3K pathway determines cisplatin resistance in ovarian cancer cells. Genetic data already provided evidence for a role of the PI3K pathway in the etiology of ovarian cancer as components of this pathway are mutated, amplified, or aberrantly expressed in ovarian cancer tissue. For example, *PI3KCA* is implicated as an oncogene in ovarian cancer (44), and *PIK3R1* is constitutively activated by mutations (45). We have found that elevated levels of *PIK3R2* expression negatively affect outcome in patients with ovarian cancer. *AKT2* is amplified in 12% of ovarian carcinomas (46), and it was reported that AKT2 provokes cisplatin resistance in ovarian cancer cells (47). We have found that *AKT2* expression has a negative correlation with overall survival of patients with ovarian cancer.

Therapeutic perspectives. It can be concluded from these results that the IGF-IR and PI3K signaling pathways are of immediate importance for the therapy of cisplatin-resistant ovarian carcinomas. Because IGF-I mediates a bystander effect for cisplatin resistance, it is a meaningful strategy to target the IGF-IR or PI3K to improve the efficacy of platinum based chemotherapy. As the PI3K pathway is also activated in ovarian carcinomas, it might be a promising strategy to use a combination therapy that targets the IGF-IR on the one hand and components of the PI3K pathway on the other. A variety of IGF-IR and PI3K inhibitors are used in clinical trials for the therapy of diverse cancers (48, 49). It is also feasible to target downstream components of the PI3K pathway. For example RAD001 (everolimus) targets mammalian target of rapamycin, which is required for AKT phosphorylation on Ser^{473} (19). RAD001 inhibits human ovarian cancer cell proliferation, enhances cisplatin-induced apoptosis, and prolongs survival in an ovarian cancer model (50). RAD001 is used in a large variety of clinical studies[7] aimed at treating diverse malignant diseases. We envision that our results will translate into the clinic and aid to develop novel therapies targeting the IGF-IR and PI3K pathways in ovarian cancer.

[7] http://clinicaltrials.gov

Disclosure of Potential Conflicts of Interest

No potential conflicts of interest were disclosed.

Acknowledgments

Received 8/14/08; revised 12/19/08; accepted 1/19/09; published OnlineFirst 3/24/09.

Grant support: Intramural funding of the caesar foundation (H.D. Royer).

The costs of publication of this article were defrayed in part by the payment of page charges. This article must therefore be hereby marked *advertisement* in accordance with 18 U.S.C. Section 1734 solely to indicate this fact.

We thank V. Riehmer (caesar) for skillful technical assistance, Hernando (Womans Hospital, Bonn) for providing ovarian cancer cell lines.

References

1. Ozols RF, Bookman MA, Connolly DC, et al. Focus on epithelial ovarian cancer. Cancer Cell 2004;5:9–24.
2. Aabo K, Adams M, Adnitt P, et al.; Advanced Ovarian Cancer Trialists' Group. Chemotherapy in advanced ovarian cancer: four systematic meta-analyses of individual patient data from 37 randomized trials. Br J Cancer 1998;78:1479–87.
3. Cannistra SA. Cancer of the ovary. N Engl J Med 2004;351:2519–29.
4. Wang D, Lippard SJ. Cellular processing of platinum anticancer drugs. Nat Rev Drug Discov 2005;4:307–20.

5. Stewart DJ. Mechanisms of resistance to cisplatin and carboplatin. Crit Rev Oncol Hematol 2007;63:12–31.
6. Markman M. The promise and perils of 'targeted therapy' of advanced ovarian cancer. Oncology 2008;74:1–6.
7. Eckstein N, Servan K, Girard L, et al. Epidermal growth factor receptor pathway analysis identifies amphiregulin as a key factor for cisplatin resistance of human breast cancer cells. J Biol Chem 2008;283:739–50.
8. Eva A, Robbins KC, Andersen PR, et al. Cellular genes analogous to retroviral onc genes are transcribed in human tumour cells. Nature 1982;295:116–9.
9. Behrens BC, Hamilton TC, Masuda H, et al. Characterization of a cis-diamminedichloroplatinum(II)-resistant human ovarian cancer cell line and its use in evaluation of platinum analogues. Cancer Res 1987;47:414–8.
10. Brown R, Clugston C, Burns P, et al. Increased accumulation of p53 protein in cisplatin-resistant ovarian cell lines. Int J Cancer 1993;55:678–84.
11. Holford J, Rogers P, Kelland LR. ras mutation and platinum resistance in human ovarian carcinomas *in vitro*. Int J Cancer 1998;77:94–100.
12. Mitelman F, editor. An International System for Human Cytogenetic Nomenclature. Basel: Karger; 1995.
13. Trost D, Hildebrandt B, Beier M, Muller N, Germing U, Royer-Pokora B. Molecular cytogenetic profiling of complex karyotypes in primary myelodysplastic syndromes and acute myeloid leukemia. Cancer Genet Cytogenet 2006;165:51–63.
14. Knight SJ, Lese CM, Precht KS, et al. An optimized set of human telomere clones for studying telomere integrity and architecture. Am J Hum Genet 2000;67:320–32.
15. Evers C, Beier M, Poelitz A, et al. Molecular definition of chromosome arm 5q deletion end points and detection of hidden aberrations in patients with myelodysplastic syndromes and isolated del(5q) using oligonucleotide array CGH. Genes Chromosomes Cancer 2007;46:1119–28.
16. Hupe P, Stransky N, Thiery JP, Radvanyi F, Barillot E. Analysis of array CGH data: from signal ratio to gain and loss of DNA regions. Bioinformatics 2004;20:3413–22.
17. Pollak MN, Schernhammer ES, Hankinson SE. Insulin-like growth factors and neoplasia. Nat Rev Cancer 2004;4:505–18.
18. Kyriakis JM, Avruch J. Mammalian mitogen-activated protein kinase signal transduction pathways activated by stress and inflammation. Physiol Rev 2001;81:807–69.
19. Sarbassov DD, Guertin DA, Ali SM, Sabatini DM. Phosphorylation and regulation of Akt/PKB by the rictor-mTOR complex. Science 2005;307:1098–101.
20. Durai R, Davies M, Yang W, et al. Biology of insulin-like growth factor binding protein-4 and its role in cancer [review]. Int J Oncol 2006;28:1317–25.
21. Schilder RJ, Hall L, Monks A, et al. Metallothionein gene expression and resistance to cisplatin in human ovarian cancer. Int J Cancer 1990;15:416–22.
22. Petru E, Sevin BU, Perras J, et al. Comparative chemosensitivity profiles in four human ovarian carcinoma cell lines measuring ATP bioluminiscence. Gynecol Oncol 1990;38:155–60.
23. Buick RN, Pullano R, Trent JM. Comparative properties of five human ovarian adenocarcinoma cell lines. Cancer Res 1985;45:3668–76.
24. Geisinger KR, Kute TE, Pettenati MJ, et al. Characterization of a human ovarian carcinoma cell line with estrogen and progesterone receptors. Cancer 1989;63:280–8.
25. Baldwin WS, Curtis SW, Cauthen CA, Risinger JI, Korach KS, Barrett JC. BG-1 ovarian cell line: an alternative model for examining estrogen-dependent growth *in vitro*. In vitro Cell Dev Biol Anim 1998;34:649–54.
26. Dressman HK, Berchuck A, Chan G, et al. An integrated genomic-based approach to individualized treatment of patients with advanced-stage ovarian cancer. J Clin Oncol 2007;25:517–25.
27. Sawyers CL. The cancer biomarker problem. Nature 2008;452:548–52.
28. Prasad M, Bernardini M, Tsalenko A, et al. High definition cytogenetics and oligonucleotide aCGH analyses of cisplatin-resistant ovarian cancer cells. Genes Chromosomes Cancer 2008;47:427–36.
29. Auersperg N, Wong AS, Choi KC, Kang SK, Leung PC. Ovarian surface epithelium: biology, endocrinology, and pathology. Endocr Rev 2001;22:255–88.
30. Kuroda H, Mandai M, Konishi I, et al. Human chorionic gonadotropin (hCG) inhibits cisplatin-induced apoptosis in ovarian cancer cells: possible role of up-regulation of insulin-like growth factor-1 by hCG. Int J Cancer 1998;76:571–8.
31. Poretsky L, Cataldo NA, Rosenwaks Z, Giudice LC. The insulin-related ovarian regulatory system in health and disease. Endocr Rev 1999;20:535–82.
32. Kalli KR, Conover CA. The insulin-like growth factor/insulin system in epithelial ovarian cancer. Front Biosci 2003;8:d714–22.
33. Hamilton TC, Young RC, McKoy WM, et al. Characterization of a human ovarian carcinoma cell line (NIH:OVCAR-3) with androgen and estrogen receptors. Cancer Res 1983;43:5379–89.
34. Resnicoff M, Ambrose D, Coppola D, Rubin R. Insulin-like growth factor-1 and its receptor mediate the autocrine proliferation of human ovarian carcinoma cell lines. Lab Invest 1993;69:756–60.
35. Selvakumaran M, Pisarcik DA, Bao R, Yeung AT, Hamilton TC. Enhanced cisplatin cytotoxicity by disturbing the nucleotide excision repair pathway in ovarian cancer cell lines. Cancer Res 2003;63:1311–6.
36. Gotlieb WH, Bruchim I, Gu J, et al. Insulin-like growth factor receptor I targeting in epithelial ovarian cancer. Gynecol Oncol 2005;100:389–96.
37. Burke F, Relf M, Negus R, Balkwill F. A cytokine profile of normal and malignant ovary. Cytokine 1996;8:578–85.
38. Berns EM, Klijn JG, Henzen-Logmans SC, et al. Receptors for hormones and growth factors and (onco)-gene amplification in human ovarian cancer. Int J Cancer 1992;52:218–24.
39. van Dam PA, Vergote IB, Lowe DG, et al. Expression of c-erbB-2, c-myc, and c-ras oncoproteins, insulin-like growth factor receptor, and epidermal growth factor receptor in ovarian carcinoma. J Clin Pathol 1994;47:914–9.
40. Karasik A, Menczer J, Pariente C, Kanety H. Insulin-like growth factor-I (IGF-I) and IGF-binding protein-2 are increased in cyst fluids of epithelial ovarian cancer. J Clin Endocrinol Metabol 1994;78:271–6.
41. Na Yj, Kim KT, Yoo JB, Moon H, Hwang YY, Shin JH. Significance of insulin-like growth factor-1 (IGF-1) in the ascites of ovarian cancer. Korean J Gynecol Oncol Colposc 1995;6:227–34.
42. Spentzos D, Cannistra SA, Grall F, et al. IGF axis gene expression patterns are prognostic of survival in epithelial ovarian cancer. Endocr Relat Cancer 2007;14:781–90.
43. Brokaw J, Katsaros D, Wiley A, et al. IGF-I in epithelial ovarian cancer and its role in disease progression. Growth Factors 2007;25:346–54.
44. Shayesteh L, Lu Y, Kuo WL, et al. PIK3CA is implicated as an oncogene in ovarian cancer. Nat Genet 1999;21:99–102.
45. Levine DA, Bogomolniy F, Yee CJ, et al. Frequent mutation of the PIK3CA gene in ovarian and breast cancers. Clin Cancer Res 2005;11:2875–8.
46. Bellacosa A, de Feo D, Godwin AK, et al. Molecular alterations of the AKT2 oncogene in ovarian and breast carcinomas. Int J Cancer 1995;64:280–5.
47. Yuan ZQ, Feldman RI, Sussman GE, Coppola D, Nicosia SV, Cheng JQ. AKT2 inhibition of cisplatin-induced JNK/p38 and Bax activation by phosphorylation of ASK1: implication of AKT2 in chemoresistance. J Biol Chem 2003;278:23432–40.
48. Weroha SJ, Haluska P. IGF-1 receptor inhibitors in clinical trials - early lessons. J Mammary Gland Biol Neoplasia 2008;13:471–83.
49. Marone R, Cmiljanovic V, Giese B, Wymann MP. Targeting phosphoinositide 3-kinase - moving towards therapy. Biochim Biophys Acta 2008;1784:159–85.
50. Mabuchi S, Altomare DA, Cheung M, et al. RAD001 inhibits human ovarian cancer cell proliferation, enhances cisplatin-induced apoptosis, and prolongs survival in an ovarian cancer model. Clin Cancer Res 2007;13:4261–70.